PHYSICAL REVIEW B **82**, 180506(R) (2010)

Properties of vacancy formation in hcp ^{4}He crystals at zero temperature and fixed pressure

Y. Lutsyshyn,[1,*] C. Cazorla,[2] G. E. Astrakharchik,[1] and J. Boronat[1]
[1]*Departament de Física i Enginyeria Nuclear, Universitat Politècnica de Catalunya, Campus Nord B4-B5, E-08034 Barcelona, Spain*
[2]*Department of Chemistry, University College London, London WC1H 0AJ, United Kingdom*
(Received 9 August 2010; published 4 November 2010)

Equation of state of ^{4}He hcp crystals with vacancies is determined at zero temperature using the diffusion Monte Carlo technique, an exact ground-state zero-temperature method. This allows us to extract the formation enthalpy and isobaric formation energy of a single vacancy in otherwise perfect helium solid. Results are obtained for pressures up to 160 bar. The isobaric formation energy is found to reach a minimum near 57 bar where it is equal to 10.5 ± 1.2 K. At the same pressure, the vacancy formation volume exhibits a maximum and reaches the volume of the unit cell. This pressure coincides with the pressure interval over which a peak in the supersolid fraction of ^{4}He was observed in a recent experiment.

DOI: 10.1103/PhysRevB.82.180506 PACS number(s): 67.80.−s, 61.72.J−

Properties of solid ^{4}He have regained interest since the discovery that it exhibits nonclassical moment of inertia[1] and several accompanying phenomena (for a review, see Refs. 2–4). Recently, Kim and Chan[5] studied torsional oscillator response as a function of pressure. A large fraction of sample growth (about one half) in that study was completed at fixed pressure. Kim and Chan found that the supersolid fraction changed threefold over the studied pressure range (up to 135 bar) and had a distinct maximum at pressures near 55 bar, which is well above melting pressure. These results call for a study of possible supersolidity mechanisms under isobaric conditions.

Crystal defects are believed to be indispensable in the mechanisms behind supersolidity.[2,6] In particular, special attention has been paid in the past to vacancy defects. Unbound vacancies, whether intrinsic to solid helium or introduced by experimental conditions, are likely to cause supersolidity.[4,7] Experimental results for energy of vacancy formation in pure ^{4}He are available from the work of Fraass *et al.*[8] with additional data and analysis by Blackburn and colleagues.[9] Numerous theoretical works describe vacancies in solid helium.[7,10–18] Results for vacancy formation energy are available from finite-temperature calculations using path-integral Monte Carlo methods[14,15] and from ground-state calculations with variational,[11–13,17] shadow path-integral ground state,[17] and diffusion[7] Monte Carlo methods. These calculations agree that individual vacancies cost too much energy to exist in the ground state of solid helium. However, properties of isobaric vacancy formation in ^{4}He have not yet been reported. Additionally, several important vacancy properties, such as vacancy volume, are only sensible if considered at fixed pressure. To address these concerns, we performed a calculation of the equation of state of solid ^{4}He with the number of atoms incommensurate with the number of sites of an hcp lattice filling the volume. Incommensurate in this sense, the solid remained crystalline and had one vacancy defect per (periodic) simulation volume. Obtaining such an equation of state allowed us to extract the dependence of vacancy properties computed at both fixed pressure and fixed density conditions. Importantly, calculated formation energy at fixed pressure is considerably smaller than the formation energy at fixed density. It also turned out to exhibit a minimum around the same pressure where a peak in the supersolid response was observed experimentally.

The most important thermodynamic quantity characterizing the presence of vacancies in fixed-pressure systems is the Gibbs free energy,[19] which at zero temperature reduces to enthalpy. Consider the enthalpy $H(N,0,P)$ of a commensurate system consisting of N particles at pressure P and $H(N-1,1,P)$, the enthalpy of an incommensurate system with $N-1$ particles and one vacancy at the same pressure P. If h is the enthalpy per particle and h_{vac} the vacancy formation enthalpy, then $H(N,0,P)=Nh(P)$ and $H(N-1,1,P)=(N-1)h(P)+h_{\mathrm{vac}}(P)$. The vacancy formation enthalpy in a solid can therefore be expressed as[20]

$$h_{\mathrm{vac}}(P) = H(N-1,1,P) - \frac{N-1}{N}H(N,0,P)$$
$$= E(N-1,1,P) - \frac{N-1}{N}E(N,0,P)$$
$$+ (N-1)P\left[\frac{1}{\rho_{\mathrm{inc}}} - \frac{1}{\rho_{\mathrm{com}}}\right], \quad (1)$$

where ρ_{inc} and ρ_{com} are the densities of the incommensurate and commensurate systems at pressure P. Pressure can be obtained from the derivative of the energy with respect to the density ρ as

$$P = \rho^2 \frac{\partial E/N}{\partial \rho} \quad (2)$$

thus allowing us to obtain $E(P)$ and $\rho(P)$ from the $E(\rho)$ dependence available from the calculations.

The isobaric vacancy formation energy ΔE_P is the energy cost of moving a single atom away from a lattice site while keeping the pressure fixed

$$\Delta E_P = E(N-1,1,P) - \frac{N-1}{N}E(N,0,P). \quad (3)$$

ΔE_P determines the formation enthalpy with the addition of the work necessary to free the vacancy volume Ω_{vac}, via $h_{\mathrm{vac}}=\Delta E_P + P\Omega_{\mathrm{vac}}$. The incommensurate system has an excess of volume with regard to its number of atoms. It can be

written as $V(N-1,1,P)=(N-1)v+\Omega_{\rm vac}$, where v is the volume normally occupied per particle, $V(N,0,P)=Nv$. Hence the vacancy volume can be obtained from

$$\Omega_{\rm vac} = V(N-1,1,P) - \frac{N-1}{N}V(N,0,P). \tag{4}$$

In previously published numerical simulations, the formation energy was calculated at *fixed density* as

$$\Delta E_\rho = E(N-1,1,\rho) - \frac{N-1}{N}E(N,0,\rho), \tag{5}$$

which compares two systems with volume adjusted to provide equal densities. While ΔE_ρ matches ΔE_P at *zero* pressure,[21] they generally differ at nonzero pressures necessary to solidify helium. In fact, at zero temperature ΔE_ρ slowly approaches $h_{\rm vac}$ in the thermodynamic limit: $h_{\rm vac}-\Delta E_\rho \propto 1/N$.[22,23] Attempting to obtain $h_{\rm vac}$ from ΔE_ρ is thus subject to strong finite-size effects even if $h_{\rm vac}$ itself converges quickly.

Calculations were made with diffusion Monte Carlo (DMC), a statistically exact ground-state method. DMC has proven indispensable in understanding properties of superfluid ^{4}He and yields excellent results for the properties of solid ^{4}He,[7,24] in particular, for the equation of state. DMC projects the excited states from the initial conditions $\phi_{\rm I}$ by advancing through imaginary time τ a function $f=\phi_{\rm G}\exp[-(H-E_0)\tau]\phi_{\rm I}$, where H is the Hamiltonian, E_0 is a reference energy and $\phi_{\rm G}$ is an importance sampling function, also called guiding wave function. For details of the method, see Refs. 25–27. Interactions were modeled with the Aziz HFD-B(HE) potential.[28] While this potential is known to produce a slight systematic bias in energy of under 70 mK, it allows for a good reproduction of the equation of state $P(\rho)$.[24,26]

A good-quality guiding wave function $\phi_{\rm G}$ is necessary to efficiently sample the energy from the ground state itself. Such a wave function has to take into account two-body correlations between atoms, to provide lattice symmetry, to allow for hopping between lattice sites, and finally it needs to satisfy the Bose symmetry. We used a symmetrized form of the Nosanow-Jastrow[29] wave function that was recently developed for quantum solids[7] and has the form

$$\phi_{\rm SNJ} = \left[\prod_{i<j}^{N_{\rm p}} f(|\boldsymbol{r}_i-\boldsymbol{r}_j|)\right]\left[\prod_{k}^{N_{\rm s}}\sum_{i}^{N_{\rm p}} g(|\boldsymbol{r}_i-\boldsymbol{l}_k|)\right], \tag{6}$$

where $N_{\rm p}$ and $N_{\rm s}$ are, respectively, the number of atoms and lattice sites, $f(r)$ is the pair-correlation function and $g(r)$ is a function that localizes atoms to the lattice sites. $|\boldsymbol{r}_i-\boldsymbol{l}_k|$ denotes distance from an atom with index i to the lattice site k. $\phi_{\rm SNJ}$ is both Bose-symmetric and provides an excellent spatial order.[7] We used $g(r)=\exp[-1/2\gamma r^2]$ and the McMillan form $f(r)=\exp[-1/2(b/r)^5]$. The parameters were obtained from variational optimization of the Nosanow-Jastrow wave function, resulting in $b=1.12\sigma$, where $\sigma=2.556$ Å and $\gamma=(-6.210+27.69\rho\sigma^3)/\sqrt{\sigma}$. Stability was observed for changes in timestep, population size, and wave-function parameters over the entire range of densities.

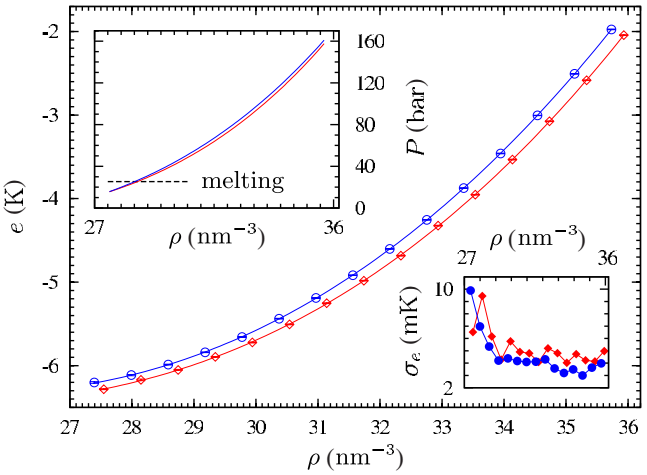

FIG. 1. (Color online) Energy per particle of the commensurate system (◇) and the incommensurate system with one of the 180 sites being vacant (○). Error bars are smaller than the symbols and are shown within them. Solid lines in the main plot area are third-degree polynomial fits as described in the text. Lower inset separately shows statistical errors with solid symbols. Top inset shows pressures for both systems (pressure of the incommensurate solid is higher). Dashed line marks melting pressure, below which both systems are metastable but remain crystalline.

The commensurate solid was simulated by considering a periodic system with 180 atoms in a volume containing 180 hcp lattice sites. This number allows for an efficient simulation using nearly cubic geometry with ratio of sides of the simulation box equal to 1.06:1.02:1. The incommensurate crystal was simulated by using one less atom while keeping the lattice intact. Separate calculations using nonorthorhombic simulation volumes convince us that the particular shape of the cell does not influence the results so long as the simulated system is large enough in the smallest dimension, and the system has the desired relation between the number of atoms and available lattice sites. Size effects resulting from finite simulation box size were compensated by separate variational calculations involving up to 1440 atoms with the methodology of Ref. 30 but with the inclusion of $(1/N)^2$ terms. Vacancy images created by periodic boundary conditions are sufficiently separated to neglect their interaction.[31]

The results for the equation of state of both commensurate and incommensurate systems are presented in Fig. 1. The resulting density dependence of energy per particle $e(\rho)$ could be fitted accurately with third-degree polynomials, which in this case are equivalent to the form

$$e = e_0 + b(\rho/\rho_0 - 1)^2 + c(\rho/\rho_0 - 1)^3 \tag{7}$$

with the coefficients as follows: for the commensurate system, $\rho_0=25.15$ nm^{-3}, $e_0=-6.45$ K, $b=17.3$ K, and $c=15.7$ K; for the system with a vacancy, $\rho_0=25.51$ nm^{-3}, $e_0=-6.34$ K, $b=22.5$ K, and $c=11.7$ K. From the dependence of energy on density, we can extract the formation properties according to Eqs. (1)–(5). To accurately calculate the standard deviation in the quantities calculated from $e(\rho)$, we studied the distribution of each such quantity as deter-

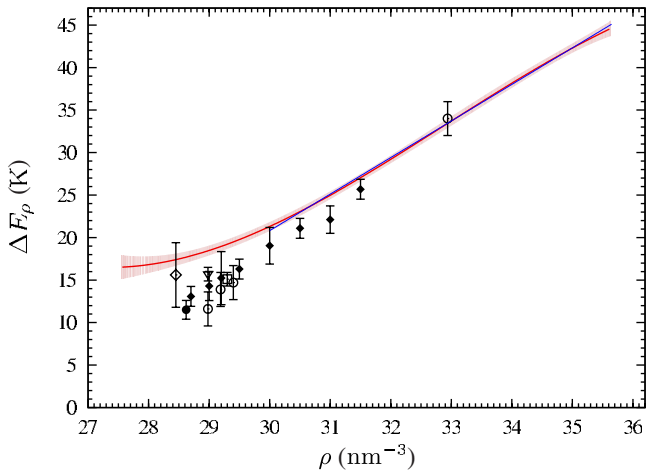

FIG. 2. (Color online) Formation energy of a vacancy at fixed density, as defined by Eq. (5). Energy is shown with the solid line while the area within one standard deviation is shaded. The straight line shows the fit at high densities. Symbols show numerical data from Ref. 11 (○), Ref. 12 (◇), Ref. 13 (▽), Ref. 17 (□), Ref. 15 (●), and Ref. 14 (◆).

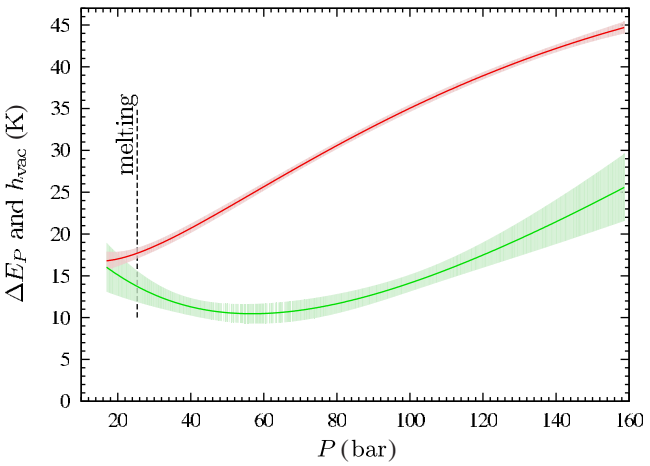

FIG. 3. (Color online) Vacancy formation enthalpy (red, upper curve) and isobaric formation energy (green, lower curve). Shaded areas mark one standard deviation. Dashed line shows melting pressure.

mined directly by the statistical errors in the calculation of the energy values.

Vacancy formation energy at fixed density, computed according to Eq. (5), is shown in Fig. 2. At large densities, ΔE_ρ grows nearly linearly. The apparent bending at highest considered densities is not discernible within the current error levels. For densities ρ above 30 nm^{-3}, ΔE_ρ can be approximated within 0.5 K as $\Delta E_\rho = k(\rho/\rho_r - 1)$ with $k = 108.2$ K and $\rho_r = 25.16$ nm^{-3}. It is notable that ΔE_ρ approaches a plateau at low densities. The lowest value $\Delta E_\rho = 16.5 \pm 1.4$ K is reached at the lowest studied density of $\rho = 27.6$ nm^{-3}. Fixed-density formation energies obtained by other groups are also plotted for comparison in Fig. 2. Our values are higher over a range of densities close to melting. The reasons for this discrepancy are unclear.

By matching the pressure between the systems with a vacancy and without any, we were able to compute the vacancy formation enthalpy and the isobaric formation energy, shown in Fig. 3. One may compare the results to the experimental data of Fraass *et al.*,[8] considering them at the reported pressure at which the growth process was performed (two such experimental points are available). It is a curious coincidence that the experimental results coincide with our calculated values of the isobaric energy of vacancy formation and not with the enthalpy. Samples of that experiment were reported as grown at constant pressure, however, the experiment itself was reported to be performed at fixed volume.

The minimum that we find in ΔE_P is unexpected and is not observed in classical solids.[20] Expanding the equation of state of the system with one vacancy around density ρ, one obtains

$$\Delta E_P^{\text{approx}}(P) = \Delta E_\rho(\rho) - (N-1)\beta_{\text{inc}} P \frac{\Delta P}{\rho} + \mathcal{O}\left(\frac{1}{N}\right),$$

where $\Delta P = P_{\text{inc}}(\rho) - P_{\text{com}}(\rho)$ is the difference in pressure between the two systems, β_{inc} is the compressibility of the incommensurate system and $P = P_{\text{com}}(\rho)$. Using the quantities obtained from our calculations, we find that $\Delta E_P^{\text{approx}}$ matches the result for ΔE_P to within 1 K, including the minimum structure. The minimum in ΔE_P occurs around the pressure of 57 bar, where the energy lowers to 10.5 ± 1.2 K. This pressure is coincidentally rather close to the value where Kim and Chan[5] observed a maximum in the supersolid fraction. Unlike for energy, there is not an extremum in vacancy formation enthalpy. The minimum in energy is balanced by the character of the dependence of vacancy volume on pressure. Nonetheless, the second derivative of h_{vac} changes sign around this pressure.

The vacancy formation volume Ω_{vac}, shown in Fig. 4, is also nonmonotonic and reaches a maximum at 57 bar while its volume in relation to the unit-cell volume of the incommensurate system v_{lat} peaks at 63 bar (see left inset in Fig. 4; statistical uncertainty does not allow us to distinguish

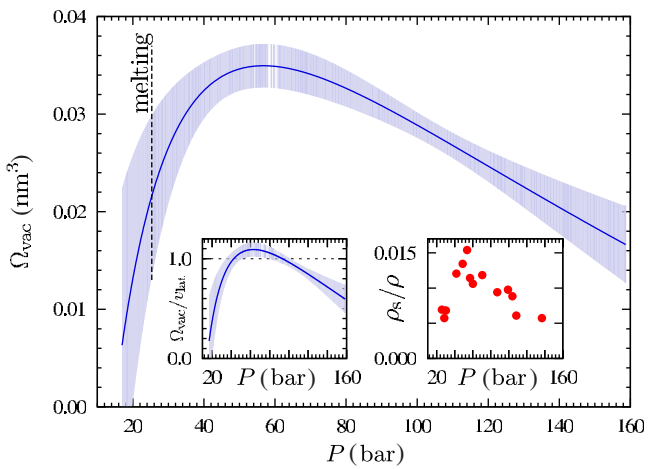

FIG. 4. (Color online) Vacancy formation volume as a function of pressure [Eq. (4)]. Shaded area indicates statistical error. The curve peaks at $P = 57$ bar. The left inset shows formation volume of vacancy relative to the volume of the unit cell while the inset on the right shows the experimental supersolid fraction from Ref. 5.

whether Ω_{vac} indeed peaks above v_{lat}). Not only the peak location but also the overall shape of $\Omega_{vac}(P)$ strikingly resembles the pressure dependence of the supersolid fraction as measured by Kim and Chan[5] (shown for comparison on the right inset of Fig. 4). While we do not have a rigorous explanation for this coincidence, it is worth noting that the peak value of Ω_{vac} is close to v_{lat}. Consider some volume $V=L^3$ surrounding a vacancy. To ensure the correct value of $\Omega_{vac}-v_{lat}$, the deformation of lattice lines on the border of this imaginary volume has to scale as $(\Omega_{vac}-v_{lat})/L^2$. Therefore, the strain on the border of this volume is proportional to $(\Omega_{vac}-v_{lat})v_{lat}^{1/3}/V$. Volume encompassing a region with the strain above some threshold ε_c is given by $V_c \propto (\Omega_{vac}-v_{lat})v_{lat}^{1/3}/\varepsilon_c$. This means that the volume of the strained region of the lattice that accompanies a vacant lattice site in solid helium is strongly reduced at pressures close to 60 bar.

To conclude, we have been able to characterize the isobaric vacancy formation in solid ^{4}He. Thermodynamic vacancy properties were extracted from the calculations of the equations of state of solid helium with number of atoms both commensurate and incommensurate with the number of available atomic sites. Isobaric vacancy formation energy turned out to be significantly lower than the energy of formation at fixed density. The value of the isobaric formation energy is nonetheless high enough to exclude the possibility of intrinsic noninteracting vacancies in the supersolid experiments. However, we find a strong resemblance between the pressure dependence of vacancy formation volume and experimental results for the supersolid fraction. The maximum in the formation volume is accompanied by a formation energy minimum at the same pressure. These coincidences suggest that vacancies may be in fact in some way involved in the supersolidity mechanisms.

Authors would like to thank Mike Gillan and Moses Chan for helpful discussions. This work was partially supported by DGI (Spain) under Grant No. FIS2008-04403 and Generalitat de Catalunya under Grant No. 2009SGR-1003.

*yaroslav.lutsyshyn@upc.edu

[1] E. Kim and M. H. W. Chan, Nature (London) **427**, 225 (2004).
[2] N. Prokof'ev, Adv. Phys. **56**, 381 (2007).
[3] D. E. Galli and L. Reatto, J. Phys. Soc. Jpn. **77**, 111010 (2008).
[4] S. Balibar, and F. Caupin, J. Phys.: Condens. Matter **20**, 173201 (2008).
[5] E. Kim and M. H. W. Chan, Phys. Rev. Lett. **97**, 115302 (2006).
[6] N. Prokof'ev and B. Svistunov, Phys. Rev. Lett. **94**, 155302 (2005).
[7] C. Cazorla, G. E. Astrakharchik, J. Casulleras, and J. Boronat, New J. Phys. **11**, 013047 (2009).
[8] B. A. Fraass, P. R. Granfors, and R. O. Simmons, Phys. Rev. B **39**, 124 (1989).
[9] E. Blackburn, J. M. Goodkind, S. K. Sinha, J. Hudis, C. Broholm, J. van Duijn, C. D. Frost, O. Kirichek, and R. B. E. Down, Phys. Rev. B **76**, 024523 (2007).
[10] D. M. Ceperley and B. Bernu, Phys. Rev. Lett. **93**, 155303 (2004).
[11] F. Pederiva, G. V. Chester, S. Fantoni, and L. Reatto, Phys. Rev. B **56**, 5909 (1997).
[12] B. Chaudhuri, F. Pederiva, and G. V. Chester, Phys. Rev. B **60**, 3271 (1999).
[13] D. E. Galli and L. Reatto, J. Low Temp. Phys. **134**, 121 (2004).
[14] M. Boninsegni, A. B. Kuklov, L. Pollet, N. V. Prokof'ev, B. V. Svistunov, and M. Troyer, Phys. Rev. Lett. **97**, 080401 (2006).
[15] B. K. Clark and D. M. Ceperley, Comput. Phys. Commun. **179**, 82 (2008).
[16] L. Pollet, M. Boninsegni, A. B. Kuklov, N. V. Prokof'ev, B. V. Svistunov, and M. Troyer, Phys. Rev. Lett. **101**, 097202 (2008).
[17] M. Rossi, E. Vitali, D. E. Galli, and L. Reatto, J. Phys.: Conf. Ser. **150**, 032090 (2009).
[18] R. Pessoa, M. de Koning, and S. A. Vitiello, Phys. Rev. B **80**, 172302 (2009).
[19] N. W. Ashcroft and N. D. Mermin, *Solid State Physics* (Sounders College Publishing, Orlando, 1976).
[20] S. Mukherjee, R. E. Cohen, and O. Gülseren, J. Phys.: Condens. Matter **15**, 855 (2003).
[21] M. J. Gillan, J. Phys.: Condens. Matter **1**, 689 (1989).
[22] S. M. Heald, D. R. Baer, and R. O. Simmons, Phys. Rev. B **30**, 2531 (1984).
[23] See supplementary material at http://link.aps.org/supplemental/10.1103/PhysRevB.82.180506 for derivation.
[24] L. Vranješ, J. Boronat, J. Casulleras, and C. Cazorla, Phys. Rev. Lett. **95**, 145302 (2005).
[25] S. A. Chin, Phys. Rev. A **42**, 6991 (1990).
[26] J. Boronat and J. Casulleras, Phys. Rev. B **49**, 8920 (1994).
[27] B. L. Hammond, W. Lester, Jr., and P. J. Reynolds, *Monte Carlo Methods in Ab Initio Quantum Chemistry* (World Scientific, Singapore, 1994).
[28] R. A. Aziz, F. R. W. McCourt, and C. C. K. Wong, Mol. Phys. **61**, 1487 (1987).
[29] L. H. Nosanow, Phys. Rev. Lett. **13**, 270 (1964).
[30] C. Cazorla and J. Boronat, J. Phys.: Condens. Matter **20**, 015223 (2008).
[31] G. D. Mahan and H. Shin, Phys. Rev. B **74**, 214502 (2006).